PROCEEDINGS OF SCIENCE

Asymmetries for neutral pion photoproduction in the threshold region

David Hornidge*
Mount Allison University
E-mail: dhornidge@mta.ca

We report on two pion-photoproduction measurements in the threshold region conducted in the A2 collaboration at MAMI with the almost 4π Crystal Ball detector. The first was with a linearly polarized photon beam and unpolarized liquid-hydrogen target. The data analysis is now complete and the linearly polarized beam asymmetry along with differential cross sections provide the most stringent test to date of the predictions of Chiral Perturbation Theory and its energy region of convergence. More recently, a measurement was performed using both circularly polarized photons and a transversely polarized butanol frozen-spin target, with the goal of extracting both the target and beam-target asymmetries. From these we intend to extract πN scattering sensitive information for the first time in photo-pion reactions. This will be used to test isospin conservation and further test dynamics of chiral symmetry breaking in QCD as calculated at low energies by Chiral Perturbation Theory.

The 7th International Workshop on Chiral Dynamics
August 6–10, 2012
Jefferson Lab, Newport News, Virginia, USA

*Speaker.

PoS(CD12)070

1. Introduction

Over an extended period of time the efforts of the A2 collaboration at Mainz have been focused on accurate measurements of low-energy γN Compton scattering and pion production reactions to perform tests of Chiral Perturbation Theory (ChPT) predictions. Study of the $\gamma p \to \pi^0 p$ reaction started with the original MAMI accelerator and a small detector to observe the $\pi^0 \to \gamma\gamma$ decay [1], and then followed with increasingly more accurate experiments to obtain the relatively small cross section [2, 3]. A parallel effort was also carried out at Saskatoon [4] during this period. The Mainz work has been building up to the sensitive spin observables [3], and the present generation photopion production experiments that we are concentrating on include accurate measurements of the cross sections, polarized photon asymmetries, and polarized target and beam-target asymmetries T and F. These experiments have been carried out with circularly and linearly polarized, tagged photons and with the almost 4π Crystal Ball and TAPS detector system. They provide very stringent tests of dynamical models [5] and predictions based on chiral symmetry breaking in QCD.

2. Photon Asymmetry in $\vec{\gamma}p \to \pi^0 p$

In December 2008 we performed an investigation of the $\vec{\gamma}p \to \pi^0 p$ reaction with a linear polarized photon beam and a liquid H_2 target using the Glasgow-Mainz photon tagger and the CB-TAPS detector system in the A2 hall at MAMI. The purpose was to execute the most accurate measurement to date of the differential cross section from threshold through the Δ region, and to greatly improve our previous polarized photon asymmetry measurement [3]. Note that the detector set-up in our original measurement covered only about 30% of 4π, meaning that the detection efficiency for the two-photon channel of π^0 decay was on the order of 10%. The more recent experiment made use of the CB-TAPS set-up shown in Figure 1—covering $\approx 96\%$ of 4π—resulting in a detection efficiency for the π^0 channel of roughly 90%. This fact alone made for a large improvement in the accuracy and counting rates for the new measurement. In addition, a higher

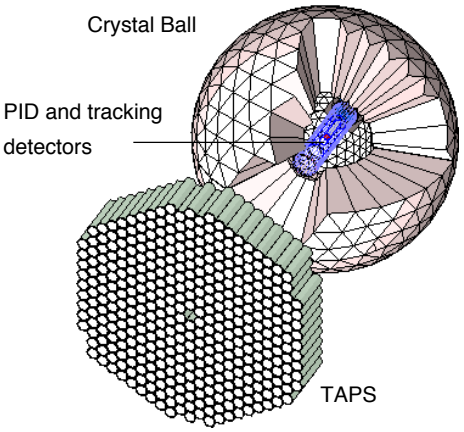

Figure 1: A cut-away view of the CB-TAPS detector system. The solid-angle coverage is approximately 96% of 4π.

energy electron beam resulted in a significant increase in the degree of polarization for the incident photon beam. The other main difference between the old and new measurements is that sufficient

empty target data was taken for the latter, which turned out to be crucial due to the contribution to the asymmetry from the 0^+ nuclei in the kapton target windows. Due to poor statistics in the older TAPS experiment, the polarized photon asymmetry, Σ, was integrated over the entire incident photon energy range, leading to data only at the cross section weighted energy average of 159.5 MeV.

For the new measurement, the data analysis is finished and sample results for the differential cross section and photon asymmetry are shown in the left column of Figure 2. The top two panels of the left column are at an incident-photon energy of 163.4 MeV as a function of pion CM production angle θ, and the bottom two are at $\theta \simeq 90 \pm 3^\circ$ as a function of incident photon energy. We have photon asymmetries from just above threshold in 2.4-MeV-wide bins, and differential cross sections from threshold into the Δ region. Fitting of the data has been done for the low-energy constants in both HBChPT [6] (solid curves in Figure 2) and relativistic ChPT [7, 8] (dashed curves in Figure 2). Moreover, with the use of an empirical model-independent partial-wave analysis, one can extract various coefficients from the differential cross sections and photon beam asymmetry, and comparisons can be made between the extracted coefficients and the theory predictions (green band in Figure 2 with error explained below). The *S*- and *P*-wave multipoles then appear only in the coefficients allowing for a direct comparison of theory and experiment.

Specifically, the differential cross section and photon asymmetry can be expanded in terms of the pion center-of-mass (CM) angle, θ, in the following way

$$\frac{d\sigma}{d\Omega}(\theta) = \frac{q}{k}\left(a_0 + a_1\cos\theta + a_2\cos^2\theta\right) \qquad \text{and} \qquad \Sigma(\theta) = \frac{q}{k}\left(b_0\sin^2\theta\right)/\frac{d\sigma}{d\Omega}(\theta)$$

where q is the CM momentum of the outgoing pion, k is the CM momentum of the incident photon, and a_0, a_1, a_2, and b_0 are the coefficients containing the *S*- and *P*-waves. In terms of the multipoles, these coefficients are given by

$$\begin{aligned} a_0 &= |E_{0^+}|^2 + P_{23}^2 & P_1 &= 3E_{1^+} + M_{1^+} - M_{1^-} \\ a_1 &= 2ReE_{0^+}P_1 & P_2 &= 3E_{1^+} - M_{1^+} + M_{1^-} \\ a_2 &= P_1^2 - P_{23}^2 & P_3 &= 2M_{1^+} + M_{1^-} \\ b_0 &= \frac{1}{2}\left(P_3^2 - P_2^2\right) & P_{23}^2 &= \frac{1}{2}(P_2^2 + P_3^2) \end{aligned}$$

Note that the *D*-waves make a contribution *even in the threshold region*, but the current data set did not have enough precision to extract them; they have been taken from the Born terms.

For the model-independent partial-wave analysis, the empirical fits to the data start with the following ansatz for the multipoles

$$E_{0^+}(W) = E_{0^+}^{(0)} + E_{0^+}^{(1)}\left(\frac{E_\gamma - E_\gamma^{\text{thr}}}{m_{\pi^+}}\right) + i\beta\frac{q_{\pi^+}}{m_{\pi^+}}, \tag{2.1}$$

$$P_i(W) = \frac{q}{m_{\pi^+}}\left[P_i^{(0)} + P_i^{(1)}\left(\frac{E_\gamma - E_\gamma^{\text{thr}}}{m_{\pi^+}}\right)\right], \tag{2.2}$$

where here E_γ and E_γ^{thr} are in the lab frame, and $E_{0^+}^{(0)}, E_{0^+}^{(1)}, P_i^{(0)}, P_i^{(1)}$ (with $i = 1,2,3$) are constants that are fit to the data.

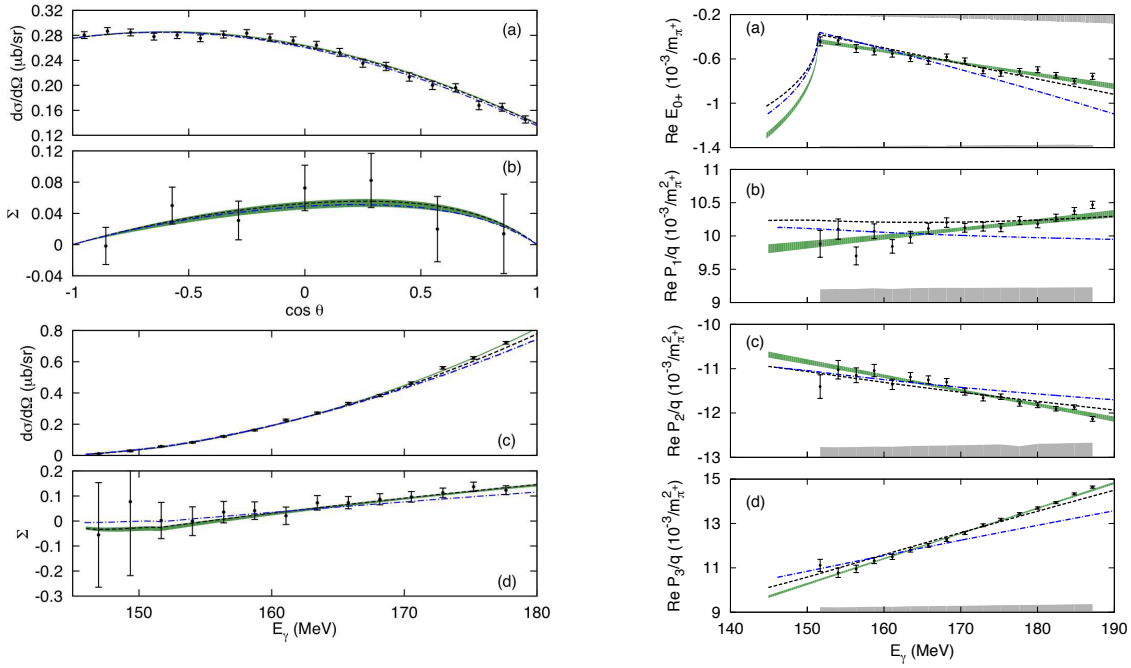

Figure 2: Left column: Differential cross sections in μb/sr (a) and photon asymmetries (b) for π^0-production as a function of pion CM production angle θ for an incident photon energy of 163.4 ± 1.2 MeV. Energy dependence of the differential cross sections (c) and photon asymmetries (d) at $\theta \simeq 90 \pm 3^\circ$. Errors shown are statistical only, without the systematic uncertainty of 4% for $d\sigma/d\Omega$ and 5% for Σ. The theory curves are dashed (black) HBChPT [6], dash-dotted (blue) relativistic ChPT [7, 8], and (green) an empirical fit with an error band. Note that in (c) and (d) the two points in incident photon energy below π^+ threshold are included. Right column: Empirical multipoles as a function of incident photon energy: (a) ReE_{0^+}, (b) ReP_1/q, (c) ReP_2/q, (d) ReP_3/q. The points are single-energy fits to the real parts of the S- and P-wave multipoles, and the empirical fits from (2.1) and (2.2) are shown with (green) statistical error bands. The $\pm$ systematic uncertainty for the single-energy extraction is represented as the gray area above the energy axis, and the systematic uncertainty in the S-wave extraction due to the uncertainty in the size of the D-wave contributions is given by the gray area at the top of (a). The theory curves are the same as in the left column.

Based on unitarity, the cusp parameter in (2.1) has the value $\beta = ReE_{0^+}(\gamma p \to \pi^+ n) a_{\rm cex}(\pi^+ n \to \pi^0 p)$ [9]. Using the best experimental value of $a_{\rm cex}(\pi^- p \to \pi^0 n) = -(0.122 \pm 0.002)/m_{\pi^+}$ obtained from the observed width in the $1s$ state of pionic hydrogen [17], assuming isospin is a good symmetry, i.e. $a_{\rm cex}(\pi^+ n \to \pi^0 p) = -a_{\rm cex}(\pi^- p \to \pi^0 n)$, and the latest measurement for $E_{0+}(\gamma p \to \pi^+ n) = (28.06 \pm 0.27 \pm 0.45) \times 10^{-3}/m_{\pi^+}$ [10], we obtain $\beta = (3.43 \pm 0.08) \times 10^{-3}/m_{\pi^+}$, which was employed in the empirical fit. The uncertainty introduced by the errors in β and isospin breaking are smaller than the statistical uncertainties of the multipole extraction depicted in Fig. 2.

The extracted multipoles are displayed in the right column of Figure 2 along with the theoretical calculations. The points are single-energy fits to the real parts of the S- and P-wave multipoles, and the energy-dependent fits from (2.1) and (2.2) are shown with the error band. The imaginary part of the S-wave multipole E_{0^+} was taken from unitarity (2.1) with the value of the cusp parameter explained above, the imaginary parts of the P-waves were assumed to be negligible, and the D-wave multipoles were calculated in the Born approximation. The impact of D-waves in the

P-wave extraction is negligible [11] but in the *S*-wave it can be sizeable. In order to assess the uncertainties in the *S*-wave extraction associated to our *D*-wave prescription we have estimated the uncertainty from the difference between the Born terms and DMT dynamical model in [5]. This error estimation is depicted in Figure 2 as a gray area at the top of the first plot. As was the case for the observables, there is very good agreement between the two ChPT calculations and the empirical values of the multipoles for energies up to $\simeq$ 160 MeV with the same pattern of deviations above that.

In conclusion, the combination of the photon asymmetry and improved accuracy in the differential cross section has allowed us to extract the real parts of the *S*-wave and all three *P*-wave multipoles as a function of photon energy for the first time. As was the case for the observables, the ChPT calculations agree with the multipoles up to an energy of $\simeq$ 165 to 175 MeV, with the relativistic calculations deviating at the lower-energy end and the HBChPT calculations closer to the upper end.

3. Target and Beam-Target Asymmetries in $\vec{\gamma}\vec{p} \to \pi^0 p$

We have performed a precise measurement of the $\vec{\gamma}\vec{p} \to \pi^0 p$ reaction from threshold to the Δ resonance using a circularly polarized photon beam and a transverse polarized target [12] to obtain the polarized target asymmetry, T, and the double polarization observable F. Note that the latter is sensitive to the *D*-wave multipoles that have recently been shown to be important in the near threshold region [11]. Preliminary asymmetries for T and F are shown in Figure 3 as both a function of angle and energy compared to numerous models predictions [5, 13, 14, 15, 16].

The target asymmetry, T, has the following form

$$T = Im E_{0^+}^{\pi^0 p}(P_3 - P_2)\sin\theta$$

which should allow us to make a direct determination of the imaginary part of the *S*-wave amplitude, $Im E_{0^+}^{\pi^0 p}$, above the $\pi^+ n$ threshold. From this, we intend to extract the cusp parameter, β, from (2.1) and then use the known value of $E_{0^+}^{\pi^+ n}$ to find $a_{ex}(\pi^+ n \to \pi^0 p)$. If isospin is conserved, then

$$a_{ex}(\pi^+ n \to \pi^0 p) = a_{ex}(\pi^- p \to \pi^0 n).$$

At the present time the right-hand side has been measured in pionic hydrogen with an error of $\simeq$ 1.5% [17], and it is anticipated that future work will reduce the uncertainty. Any deviations from the isospin conserving limit will test isospin breaking due to the electromagnetic interaction and the strong interaction due to the mass difference of the up and down quarks predicted in ChPT [18]. Observation of T for the first time in the intermediate-energy region, combined with the other accurate data which we are obtaining, will provide us with information about the πN phase shifts for charge states ($\pi^0 p, \pi^+ n$) that are not accessible to conventional πN scattering experiments. This will enable us to test isospin conservation [19]. In addition these measurements will test detailed predictions of Chiral Perturbation Theory [20] and its energy region of convergence.

References

[1] R. Beck et al., Phys. Rev. Lett. **65**, (1990) 1841–1844.

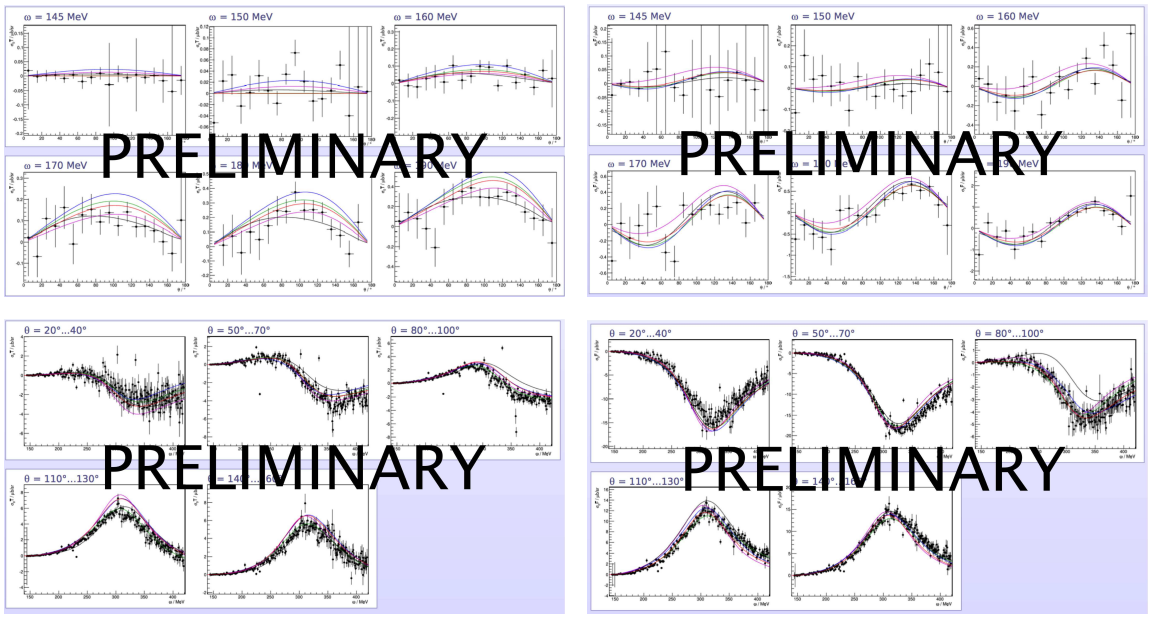

Figure 3: Preliminary target asymmetries T (left panels) and F (right panels) at six incident photon energies as a function of pion CM production angle (top panels), and for various θ bins as a function of incident photon energy (bottom panels). The errors are statistical and the lines are predictions of the DMT [5] (green), MAID [13] (red), SAID [14] (blue), Bonn-Gatchina [15] (black), and Gießen [16] (purple).

[2] M. Fuchs et al., Phys. Lett. B **368**, (1996) 20–25.

[3] A. Schmidt et al., Phys. Rev. Lett. **87**, (2001) 232501 1–4.

[4] J. C. Bergstrom et al., Phys. Rev. C **53**, (1996) R1052–R1056; Phys. Rev. C **55**, (1997) 2016–2023.

[5] S. S. Kamalov, S. N. Yang, D. Drechsel, and L. Tiator, Phys. Rev. Lett. **83**, (1999) 4494–4497; Phys. Rev. C **64**, (2001) 032201 1–5.

[6] C. Fernández-Ramírez and A. M. Bernstein, manuscript in preparation.

[7] M. Hilt, private communication.

[8] M. Hilt, S. Scherer, and L. Tiator, manuscript in preparation.

[9] A. M. Bernstein, Phys. Lett. B **442**, (1998) 20–27.

[10] E. Korkmaz et al., Phys. Rev. Lett. **83**, (1999) 3609.

[11] C. Fernández Ramírez, A. M. Bernstein, and T. W. Donnelly, Phys. Lett. B **679**, (2009) 41–44.
C. Fernández Ramírez, A. M. Bernstein, and T. W. Donnelly, Phys. Rev. C **80**, (2009) 065201 1–15.

[12] M. Ostrick, D. Hornidge, W. Deconinck, and A. M. Bernstein, spokespersons, MAMI proposal A2-10/09, (2009).

[13] D. Drechsel, O. Hanstein, S. S. Kamalov, and L. Tiator, Nucl. Phys. A **645**, (1999) 145–174; Eur. Phys. J. A **34**, (2007) 69–97.

[14] R. Arndt, W. Briscoe, I. Strakovsky, and R. Workman, Phys. Rev. C **74**, (2006) 045205.

[15] A. V. Sarantsev et al., Phys. Lett. B **659**, (2008) 94.

[16] V. Shklyar, U. Mosel, and H. Lenske, Phys. Lett. B **650**, (2007) 172.

[17] D. Gotta et al., AIP Conf. Proc. **1037**, (2008) 162–177.

[18] M. Hoferichter, B. Kubis, and U.-G. Meißner, Phys. Lett. B **678**, (2009) 65–71; Nucl. Phys. A **833**, (2010) 18–103

[19] A. M. Bernstein, πN Newsletter No. **11**, (1995), and article in preparation

[20] V. Bernard, N. Kaiser, and U.-G. Meißner, Nucl. Phys. B **383**, (1992) 442; Int. J. Mod. Phys. E **4**, (1995) 193–344; Phys. Rev. Lett. **74**, (1995) 3752–3755; Eur. Phys. J. A **11**, (2001) 209–216.